Appl. Phys. B (2014) 116:1–5
DOI 10.1007/s00340-014-5835-9

Applied Physics B
Lasers and Optics

RAPID COMMUNICATION

Near-infrared nonlinearity of a multicomponent tellurium oxide glass at 800 and 1,064 nm

Tâmara A. Oliveira · Danilo Manzani · Edilson L. Falcão-Filho · Younes Messaddeq · Georges Boudebs · Kamil Fedus · Cid B. de Araújo

Received: 11 March 2014 / Accepted: 8 April 2014 / Published online: 8 May 2014

Abstract We report on the nonlinear (NL) optical properties of glassy TeO_2–GeO_2–K_2O–Bi_2O_3 at $\lambda = 800$ nm and $\lambda = 1{,}064$ nm. Using the Kerr gate technique with a laser delivering 150 fs pulses at 800 nm, we demonstrated the fast NL response of the samples. The modulus of the NL refractive index, n_2, at 800 nm was $\sim 10^{-15}$ cm^2/W. The Z-scan technique was used to determine $n_2 \approx +10^{-15}$ cm^2/W, at 1,064 nm with pulses of 17 ps. The two-photon absorption coefficient, α_2, was smaller than the minimum that we can measure (<0.003 cm/GW). The figure of merit $n_2/\alpha_2\ \lambda$ was calculated and indicates that this glass composition has large potential to be used for all-optical switching.

1 Introduction

Heavy metal oxides (HMO) are promising materials for infrared technologies, laser devices and nonlinear (NL) photonics. Among the several HMO glasses known the tellurite glasses (TG) deserve great research efforts because of their interesting properties such as large acceptance of rare earth ions doping, low fusion temperature, high refractive index and large transmittance in the visible and infrared, and high optical third-order susceptibility, $\chi^{(3)}$. The possibility of fabrication of fibers and waveguides with strong light confinement makes TG very competitive for photonic devices.

Optical absorption, luminescence and NL optical properties of TG were investigated using several glassy compositions. Bulk glasses as well as thin amorphous films were studied in the infrared and visible range by various authors [1–19]. Recently, Stokes and anti-Stokes luminescence measurements were reported for different TG compositions doped with rare earth ions and containing metallic nanoparticles [8–12]. NL optical properties of TeO_2-based glasses were studied by various authors who reported NL refractive index $n_2 \propto Re\chi^{(3)} \sim 10^{-14}$–$10^{-15}$ cm^2/W and NL absorption coefficient $\alpha_2 \propto Im\,\chi^{(3)} \sim 10^{-1}$ cm/GW in the near-infrared [13–19]. It is known that the large nonlinearity of TG is due to the high polarizability of the Te–O bonds and the electron lone pair of the Te^{2+} ion [20, 21].

Usually, the NL susceptibility of TG may be increased by including in the glass composition compounds containing ions with lone pairs such as Bi^{3+} and Pb^{2+} or ions with unoccupied d-orbitals such as W^{6+} or Nb^{5+}. For instance, from the published results, it is clear that addition of Bi_2O_3 or Nb_2O_5 contributes to increase the value of n_2. However, in many cases, it is observed an increase in α_2 because of the optical bandgap reduction and/or because of defects or localized states inside the bandgap due to the increasing in the non-bridging oxygen ions content. These consequences cause limitation for all-optical switching applications of large number of TG compositions known.

T. A. Oliveira · E. L. Falcão-Filho · C. B. de Araújo (✉)
Departamento de Física, Universidade Federal de Pernambuco, Recife, PE 50670-901, Brazil
e-mail: cid@df.ufpe.br

D. Manzani · Y. Messaddeq
Instituto de Química, UNESP, Araraquara, SP 14801-970, Brazil

G. Boudebs · K. Fedus
Laboratoire de Photoniques d'Angers, Université d'Angers, 49045 Angers, France

K. Fedus
Institute of Physics, Nicolaus Copernicus University, Grudziadzka 5/7, 87-100 Toruń, Poland

In the present work, we report NL measurements of a multicomponent TG using lasers operating at 800 nm (pulses of 150 fs) and 1,064 nm (pulses of 17 ps). Values of n_2 and α_2 were measured for samples with different amounts of TeO_2 and Bi_2O_3 to investigate the relative contribution of these constituents for the samples' nonlinearity. In Sect. 2, we describe the samples preparation and the experimental setups used. In Sect. 3, we present the results and a discussion about the NL behavior of the samples. Finally, in Sect. 4, a summary of the results is presented.

2 Experimental

The glass samples were prepared by the conventional melt-casting method by melting the raw materials, tellurium oxide TeO_2 (3 N), germanium oxide GeO_2 (5 N), bismuth oxide Bi_2O_3 (3 N) and potassium carbonate K_2CO_3 (2 N), previously stoichiometrically weighted in order to obtain 7 g bulk glasses whose molar composition is $(80 - x)$ TeO_2–$15GeO_2$–$5K_2O$–xBi_2O_3 for $x = 5$, 10 and 15 mol%. The preparation technique was previously described in [22, 23]. First, the starting powdered materials were thoroughly mixed and load in a gold crucible. Then, the batch was melted at 760 °C during 1 h in an electrical furnace to ensure the complete elimination of CO_2 from the decomposition of the carbonate and a good homogenization and fining. Finally, the melt was cooled inside a stainless mold preheated at 20 °C below the glass transition temperature, T_g, annealed at this temperature for 2 h and slowly cooled down to room temperature to minimize residual internal stress resulting from thermal gradients upon cooling.

The introduction of GeO_2 contributes to obtain glass samples with larger thermal stability against crystallization owing the formation of a more rigid glass network. The present TG compositions were already used to fabricate microstructured optical fibers [22], as well as co-doped optical fibers for white light generation and IR emission at telecom wavelengths [23, 24].

For a better readability, the glass is labeled TGKB and the samples' compositions studied in this work as well as their T_g and the crystal transition temperature, T_x, are presented in Table 1. The TGKB samples were finally polished for the optical characterizations.

The optical absorption spectra were measured using a commercial spectrophotometer, and the linear refractive index was measured using the M-line technique.

One of the excitation sources for NL experiments was a linearly polarized mode-locked Nd: YAG laser (1,064 nm; pulses of 17 ps; 10 Hz). The measurements were performed using a Z-scan setup integrated in a 4*f*-system

Table 1 Sample parameters: composition, length, glass transition temperature (T_g) and crystallization temperature (T_x)

Sample	Composition (mol%)	Length (mm)	T_g (°C)	T_x (°C)
TGKB5	$75TeO_2$–$15GeO_2$–$5K_2O$–$5Bi_2O_3$	1.70	332	406
TGKB10	$70TeO_2$–$15GeO_2$–$5K_2O$–$10Bi_2O_3$	1.75	323	442
TGKB15	$65TeO_2$–$15GeO_2$–$5K_2O$–$15Bi_2O_3$	1.70	329	392

composed of two equal convergent lenses with focal lengths of 20 cm (see for example [25]). The image receiver at the output of the 4*f*-system is a 1,000 × 1,018 pixels cooled CCD camera (−30 °C) operating with a fixed gain. The sample is moved in the focal region along the beam propagation direction (*z*-axis). *Open-* and *closed-aperture* Z-scan normalized transmittances are numerically processed from the acquired images by integrating over all the pixels in the first case and over a circular numerical filter in the second one (corresponding to a linear aperture transmittance $S = 0.73$ in order to optimize the sensitivity and the signal-to-noise ratio [26]). The incident intensity could be adjusted by a polarizing system at the entry of the setup.

A Ti–sapphire laser (800 nm; 1.56 eV; 76 MHz; 150 fs) was used for measurements based on the Kerr gate technique [27]. The laser beam was split into two beams: pump and probe beams with intensities of 508 and 52 MW/cm^2, respectively. The sample was positioned between two crossed polarizers. The probe beam propagates along the *z*-axis, and the pump beam propagates along a direction forming a small angle with the *z*-axis. The angle between the electric fields of the pump and probe beams was set to 45°. When the pulses of the two beams overlap spatially and temporally on the sample, the pump beam induces a NL birefringence and the polarization of the probe beam rotates while propagating through the sample. Then, a fraction of the probe beam is transmitted through a polarizer/analyzer, which is oriented perpendicularly to the electric field of the incident probe beam. The signal, collected by a photodiode, is analyzed as a function of the delay time between pump and probe pulses.

3 Results and discussions

Figure 1 shows the linear absorption spectra of the samples without compensation for the Fresnel reflections on the samples' faces. It is observed a large transmittance window from 300 to 1,200 nm at room temperature. The increase in the linear absorption of sample TGKB5 in comparison with the other samples, in the proximity of the optical bandgap edge, is attributed to scattering by inhomogeneities that

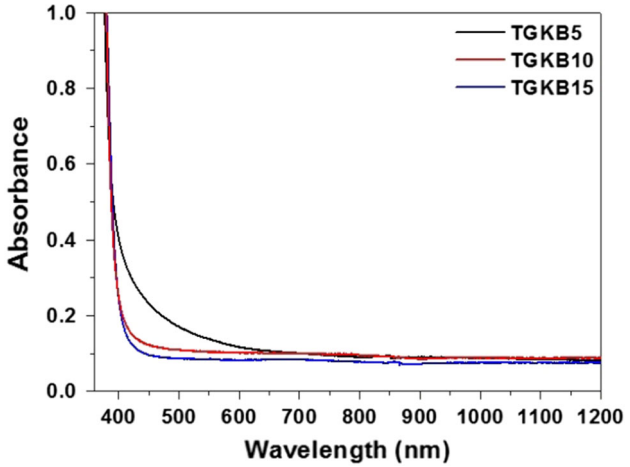

Fig. 1 Absorbance spectra. Samples' thickness: 1.70 mm (TGKB5 and TGKB15) and 1.75 mm (TGKB10)

present large scattering cross sections for smaller wavelengths due to Rayleigh scattering [22].

The linear refractive index, n_0, absorption coefficient, α_0, and optical bandgap, E_g, do not change much when the relative concentration of TeO_2 and Bi_2O_3 is changed as shown in Table 2. The large value of $n_0 \approx 2$ is attributed to the contribution of the electron lone pairs of Te^{2+} and Bi^{3+} and to their large polarizability.

The NL refractive indices were measured using the Z-scan integrated in a 4*f*-system technique [25], and Fig. 2 shows *closed-aperture* profiles that indicate positive n_2 for the three samples. The *open-aperture* experiment exhibited a NL absorption signal only for the TGKB5 sample. For the other two samples, the NL absorption signal was smaller than the minimum value that our setup can detect (0.003 cm/GW). The results, analyzed using the procedure of [28] by measuring the absolute intensity as in [29], are summarized in Table 3. If the calibration is made based on the n_2 value for CS_2 given in [28], the data in Table 3 corresponding to the 1,064 nm experiments would be larger by a factor 7.5. The choice of the measurement procedure of absolute laser intensity as derived in [29] will be justified below.

As can be seen in Table 3, the n_2 values obtained for the three samples do not differ much because the hyperpolarizabilities of TeO_2 and Bi_2O_3 have the same order of magnitude. Notice that the samples present self-focusing nonlinearity which is one order of magnitude larger than silica [30].

The large nonlinearity of the samples is due to the hyperpolarizabilities of TeO_2 and Bi_2O_3 that are due to the electron lone pairs of the Te^{2+} and Bi^{3+} ions [31–33]. The introduction of Bi_2O_3 may cause structural changes in the tellurite basic units, as discussed in [21], but the origin of the nonlinearity does not change.

Figure 3a shows the behavior of the Kerr gate signal as a function of the delay time between the pump and probe pulses at 800 nm. The symmetrical signals obtained indicate that the NL response of the samples is faster than the laser pulse duration. Monitoring the probe beam signal as a function of the pump beam intensity, we determined $6.5 \times 10^{-16} < |n_2| < 8.0 \times 10^{-16}$ cm^2/W. The measurements at 800 nm were calibrated using $n_2 = 3.1 \times 10^{-15}$ cm^2/W for CS_2, measured with 110 fs pulses [34]. Figure 3b shows the Kerr gate signal as a function of the laser intensity. The measurements showed a quadratic (linear) dependence with the pump (probe) laser intensity as expected [27]. Trials to determine α_2 by measuring the transmitted intensity as a function of the laser intensity were unsuccessful indicating that α_2 is smaller than the minimum value that our apparatus can measure (0.003 cm/GW).

The BGO model [35] was used to estimate the NL refractive index of the samples from their linear optical parameters. In this model, it is assumed that the NL polarizability is proportional to the square of the linear polarizability and the optical dispersion is due to only one resonance frequency at ω_0. The model can be applied for transparent materials when the laser frequency ω is smaller than ω_0. This condition is obeyed in the present case because the optical gap of the samples, $E_g \approx 3$ eV, is larger than the photon energies (1.56 and 1.17 eV) used in the present experiments. Moreover, the NL absorption should be negligible in comparison with NL refraction since effects such as two-photon absorption are not considered in the BGO model. For the near-infrared laser wavelengths used our samples fulfill also this criterion. Nevertheless, we add here that the last condition is probably more restrictive than it needs to be. It was already

Table 2 Indices of refraction, absorption coefficients and optical bandgaps of the samples

Sample	Index of refraction			Absorption coefficient, α_0 (cm^{-1})		Optical bandgap, E_g (eV)
	800 nm	1,064 nm	1,550 nm	800 nm	1,064 nm	
TGKB5	2.10	2.08	2.02	0.11	0.13	3.16
TGKB10	2.12	2.10	2.03	0.12	0.11	3.08
TGKB15	2.14	2.11	2.04	0.11	0.14	3.06

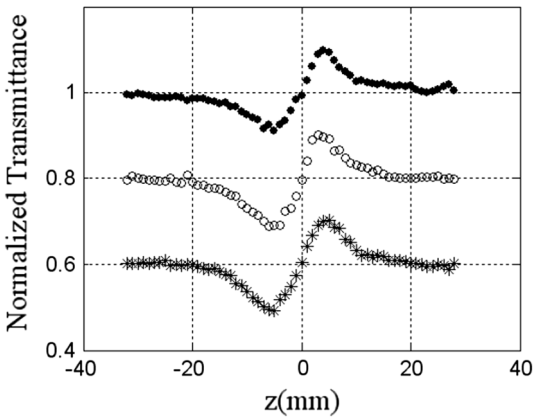

Fig. 2 Closed-aperture Z-scan profiles for excitation at 1,064 nm. Laser intensity: 7 GW/cm^2 (sample TGKB5—*solid circles*), 3 GW/cm^2 (sample TGKB10—*open circles*) and 2.9 GW/cm^2 (sample TGKB15—*asterisks*)

Table 3 Nonlinear refraction indices of the samples: experimental results and calculated values based on the BGO model

Sample	n_2 ($\times 10^{-16}$ cm^2/W)		n_2^{BGO} ($\times 10^{-16}$ cm^2/W)	
	800 nm	1,064 nm	800 nm	1,064 nm
TGKB5	6.5 ± 0.7	6.2 ± 1.52	6.6	6.2
TGKB10	8.0 ± 0.8	7.5 ± 1.2	8.1	7.5
TGKB15	7.1 ± 0.7	6.5 ± 1.2	7.2	6.7

found, studying chalcogenide glasses [34], that the BGO model predicts quite well the NL refractive indices of glass samples even when the relative magnitude of absorptive nonlinearity is 20 % of pure refractive effects (see [36] for more details).

The NL refractive index in SI units (m^2/W) may be determined by

$$n_2^{BGO} = \frac{(gS)\left[n_0^2(\lambda)+2\right]^2\left[n_0^2(\lambda)-1\right]^2}{12n_0^2(\lambda)\,c\hbar\omega_0\,(\mathrm{NS})}, \quad (1)$$

where g is a dimensionless anharmonicity parameter, S is the effective oscillator strength, c is the light speed in vacuum, $2\pi\hbar$ is the Planck's constant. $n_0(\lambda)$ is the linear refractive index at the wavelength λ and satisfies the following dispersion relation

$$\frac{n_0^2(\lambda)+2}{3n_0^2(\lambda)-1} = \frac{\omega_0^2-\omega^2}{(e^2/m\varepsilon_0)(\mathrm{NS})} \quad (2)$$

where ε_0 is the vacuum permittivity, e and m are the charge and the electron mass, respectively. Knowing $n_0(\lambda)$ for two values of λ, it is possible to determine ω_0 and (NS) and from Eq. (1) one can calculate n_2^{BGO}. The results obtained are given in Table 3 and show good agreement between the experimental and theoretical results.

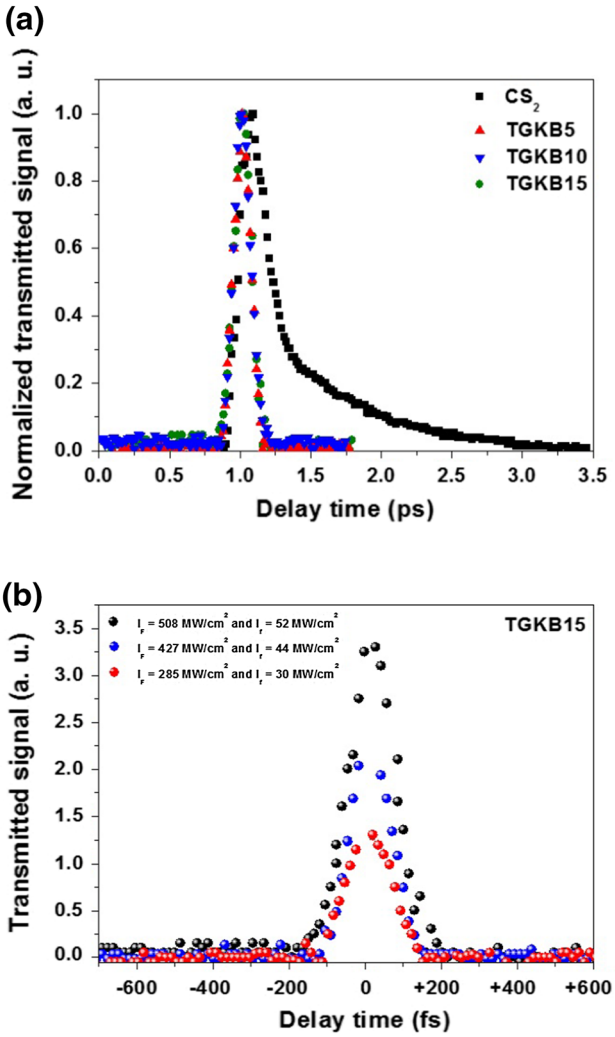

Fig. 3 **a** Kerr gate signal for excitation at 800 nm. Pump intensity: 508 MW/cm^2. Probe intensity: 52 MW/cm^2. **b** Kerr gate signal at 800 nm for different intensities (sample TGKB15). The signal obtained for CS_2 is also presented to illustrate the time response of the setup

One important point to consider here is that n_2 must present normal spectral dispersion because the laser frequencies used in the experiments were smaller than $E_g/2\pi\hbar$. Therefore, it is expected larger n_2 at 800 nm than at 1,064 nm. Nevertheless, the same order of magnitude obtained is attributed to the large detuning of both wavelengths with respect to the gap wavelength and to the different pulse durations used. It is known that the picosecond NL measurements may be affected by nuclear contributions that may contribute by 15–20 % of the total susceptibility. This reasoning justifies the choice for calibration of the present results with the procedure reported in [29]. If the present results were calibrated with basis in [28], the values of n_2 should be multiplied by 7.5 and thus the relative results for 800 and 1,064 nm would indicate anomalous dispersion of n_2.

It is important to note that the values of α_2 for both wavelengths are at least one order of magnitude smaller than the results reported for other TeO_2-based glasses. Based on the present measurements, we calculated the figures of merit for all-optical switching, $F = n_2/\alpha_2\lambda$, and we obtained $F > 1$ that indicates the possibility of using the materials for all-optical switching [37].

4 Summary

In summary, we presented measurements of n_2 and α_2 for tellurium oxide glasses containing bismuth oxide in their compositions. One relevant result was that the NL parameters in the near-infrared are equally influenced by TeO_2 and Bi_2O_3. The results show that the samples investigated present large NL refractive indices but small NL absorption coefficients. The measured parameters indicate the possibility of using the present materials for all-optical switching devices in the near-infrared.

References

1. M. Yamane, Y. Asahara, *Glasses for Photonics* (Cambridge University Press, Cambridge, 2000)
2. R.A.H. El-Mallawany, *Tellurite Glasses Handbook: Physical Properties and Data* (CRC Press, Boca Raton, 2002)
3. B. Bureau, S. Danto, H.L. Ma, C. Boussard-Plidel, X.H. Zhang, J. Lucas, Solid State Sci. **10**, 427 (2008)
4. D. Munoz-Martin, H. Fernandez, J.M. Fernandez-Navarro, J. Gonzalo, J. Solis, J.L.G. Fierro, C. Domingo, J.V. Garcia-Ramos, J. Appl. Phys. **104**, 113510 (2008)
5. K. Fedus, G. Boudebs, C.B. de Araújo, M. Cathelinaud, F. Charpentier, V. Nazabal, Appl. Phys. Lett. **94**, 061122 (2009)
6. *Processing, Properties, and Applications of Glass and Optical Materials*, ed. by A.K. Varshneya, H.A. Schaeffer, K.R. Richardson, M. Wightman, L.D. Pye (Wiley, New York, 2012)
7. A. Jha, B.D.O. Richards, G. Jose, T.T. Fernandez, C.J. Hill, J. Lousteau, P. Joshi, Int. Mater. Rev. **57**, 357 (2012)
8. G. Poirier, F.C. Cassanjes, C.B. de Araújo, V.A. Jerez, S.J.L. Ribeiro, Y. Messaddeq, M. Poulain, J. Appl. Phys. **93**, 3259 (2003)
9. V.K. Rai, L.S. Menezes, C.B. de Araújo, J. Appl. Phys. **102**, 043505 (2007)
10. R. Almeida, D.M. da Silva, L.R.P. Kassab, C.B. de Araújo, Opt. Commun. **281**, 108 (2008)
11. V.P.P. de Campos, L.R.P. Kassab, T.A.A. de Assumpção, D.S. da Silva, C.B. de Araújo, J. Appl. Phys. **112**, 063519 (2012)
12. M.S. Marques, L.D.S. Menezes, W. Lozano, L.R.P. Kassab, C.B. de Araújo, J. Appl. Phys. **113**, 053102 (2013)
13. Y. Chen, Q. Nie, T. Xu, S. Dai, X. Wang, X. Shen, J. Noncryst. Solids **354**, 3468 (2008)
14. V.K. Rai, L.S. Menzes, C.B. de Araújo, Appl. Phys. A **91**, 441 (2008)
15. E. Yousef, M. Hotzel, C. Rüssel, J. Noncryst. Solids **342**, 82 (2004)
16. E. Yousef, M. Hotzel, C. Rüssel, J. Noncryst. Solids **353**, 333 (2007)
17. L. Canioni, M.O. Martin, B. Bousquet, L. Sarger, Opt. Commun. **151**, 241 (1998)
18. S. Kim, T. Yoko, J. Am. Ceram. Soc. **78**, 1061 (1995)
19. H. Nasu, T. Uchigaki, K. Kamiya, H. Kanbara, Jpn. J. Appl. Phys. **31**, 3899 (1992)
20. M. Lines, Phys. Rev. B **43**, 11978 (1991)
21. A.P. Mirgorodsky, M. Soulis, P. Thomas, T. Merle-Méjean, M. Smirnov, Phys. Rev. B **73**, 134206 (2006)
22. D. Manzani, PhD thesis, Universidade Estadual Paulista (Araraquara, São Paulo, Brazil, 2011)
23. D. Manzani, J.L. Ferrari, F.C. Polachini, Y. Messaddeq, S.J.L. Ribeiro, J. Mater. Chem. **22**, 16540 (2012)
24. D. Manzani, Y. Ledemi, I. Skripachev, Y. Messaddeq, S.J.L. Ribeiro, R.E.P. de Oliveira, C.J.S. de Matos, Opt. Mater. Express **1**, 1515 (2011)
25. K. Fedus, G. Boudebs, Opt. Commun. **292**, 140 (2013)
26. K. Fedus, G. Boudebs, Opt. Commun. **284**, 1057 (2011)
27. R.L. Sutherland, *Handbook of Nonlinear Optics* (Wiley, New York, 1996)
28. M. Sheik-Bahae, A.A. Said, T.H. Wei, D.J. Hagan, E.W. van Stryland, IEEE J. Quantum Electron. **QE-26**, 760 (1990)
29. G. Boudebs, K. Fedus, J. Appl. Phys. **105**, 103106 (2009)
30. D. Milam, Appl. Opt. **37**, 546 (1998)
31. E. Fargin, A. Berthereau, T. Cardinal, G. Le Flem, L. Ducasse, L. Canioni, P. Segonds, L. Sarger, A. Ducasse, J. Noncryst. Solids **203**, 96 (1996)
32. C.E. Stone, A.C. Wright, R.N. Sinclair, Phys. Chem. Glasses **41**, 409 (2000)
33. L.I. Oprea, H. Hesse, K. Betzler, Opt. Mater. **26**, 235 (2004)
34. S. Couris, M. Renard, O. Faucher, B. Lavorel, R. Chaux, E. Koudoumas, X. Michaut, Chem. Phys. Lett. **369**, 318 (2003)
35. N.L. Boiling, A.J. Glass, A. Owyoung, IEEE J. Quantum Electron. **QE-26**, 760 (1990)
36. K. Fedus, G. Boudebs, Q. Coulombier, J. Troles, X.H. Zhang, J. Appl. Phys. **107**, 023108 (2010)
37. G.I. Stegeman, in *Nonlinear Optics of Organic Molecules and Polymers*, ed. by H.S. Nalva, S. Miyata (CRC, Boca Raton, 1997), p. 799